INGRID: Early Science Results

The ING's Red Imaging Device (INGRID) saw first light on the William Herschel Telescope in March 2000. In over 2 years of operation the instrument has proven to be a highly efficient infrared imager. Below we present four articles with science results from INGRID data.

Bar Strengths in Galaxies as Measured from INGRID Images

J. H. Knapen[1], D. L. Block[2], R. Buta[3], I. Puerari[4], B. G. Elmegreen[5], S. Stedman[6], D. M. Elmegreen[7]

1: ING and University of Hertfordshire; 2: University of the Witwatersrand; 3: University of Alabama; 4: INAOE; 5: IBM; 6: University of Hertfordshire; 7: Vassar College

We describe results from our study of a sample of spiral galaxies of a wide range of Hubble types on the basis of near-IR imaging obtained with INGRID on the WHT. We focus on the determination of bar torques, or bar strengths, from our images, and show that this bar strength only very weakly correlates with de Vaucouleurs bar type, or with bar axis ratio.

1. INGRID on the WHT

INGRID, the near-IR (NIR) camera for the WHT, has been in routine operation at the Cassegrain focus for almost two years now. In the three semesters from August 2000 until January 2002, it has been in scheduled use for 37, 35, and 35 nights (including NAOMI science runs, excluding commissioning and service), or 20% of the time. This makes INGRID the second-most used instrument on the WHT, after ISIS. The scientific areas that have been attacked with INGRID span an enormous range, from observational cosmology to brown dwarfs and giant planets. INGRID's main attraction is the relatively large field-of-view, of just over 4 arcmin, coupled with a pixel size of 0.24 arcsec which samples all except the very best seeing conditions. Here, we present results obtained from a number of PATT-supported observing runs, aimed at imaging nearby and relatively face-on spiral galaxies.

2. Barred Galaxies

One of the main attractions of observing in the NIR is that one is much less susceptible to the attenuation of emission by dust. Compared to the visual (*V*-band), extinction by dust is a full order of magnitude less in the NIR *K*-band, at 2.2 microns. Since at rest wavelength (i.e., in nearby galaxies) the NIR light also traces a relatively old stellar population, NIR imaging is the technique of choice to observe the "stellar backbone" of galaxies: the old stellar population which, by assumption of a mass-to-light (M/L) ratio, will give an estimate of the mass. We imaged a complete sample of 57 galaxies with INGRID for this reason: to study the old stellar component, not affected by dust extinction. In one of the lines of our overall project, the INGRID K_s imaging will be compared with *B* and *R* broad-band images, as well as with narrow-band Hα images which trace young, massive stars and current star formation. This comparison can indicate how mass and star formation are concentrated in spiral arms, and why they are concentrated to a different degree.

In this short article, though, we will focus on bars in galaxies. About 75% of all disk galaxies have bars (Sellwood & Wilkinson, 1993; Knapen, 1999), where stars move on elongated periodic orbits and thus support a non-axisymmetric potential. Gas in bars shocks and loses angular momentum, which implies that bars form a mechanism to transport material inward in a rotationally supported galactic disk. This explains why bars are relevant for questions related to the origin, evolution, and maintenance of stellar and non-stellar activity in or around the nuclei of galaxies: massive black holes, AGN or (circum)nuclear starbursts all need fuel to maintain their activity and whereas enough gas is available in the disk at large, moving this gas inwards implies making it lose a considerable amount of angular momentum.

NIR imaging is the best way of finding and classifying bars. At optical wavelengths, the bar may be masked by the combined effects of emission from young stars, and extinction by dust. There are a number of well-known and spectacular examples of bars which are unrecognisable in the visible, but well-defined in the NIR

(e.g., Block & Wainscoat, 1991; Block et al., 1994). However, statistical studies (e.g., Mulchaey & Regan, 1997; Knapen, Shlosman & Peletier, 2000; Eskridge et al., 2000) have shown that the overall bar fraction only goes up by 10–15% in the NIR as compared to classification from optical imaging. Still, the NIR is much preferred for any detailed and/or quantitative studies of bars, because the bar parameters can be measured much more cleanly there than in the optical.

3. Determining Bar Strength

Of the main structural parameters of bars: length, axis ratio, luminosity distribution, and strength, the latter has proved to be by far the most elusive observationally. Theoretically, bar strength can be defined rather easily as some measure of the ratio of non-axisymmetric, or tangential, over axisymmetric gravitational force. Observationally, bar "strength" has often been measured as bar ellipticity, or axis ratio, but this is strictly speaking incorrect. This is easy to illustrate by imagining a very elliptical bar in a galaxy which also has a massive bulge. In that case, the net gravitational pull felt by a particle (be it gaseous or stellar) in the bar will be that caused by the bar, but offset significantly by the axisymmetric gravitational pull of the bulge. Thus, the net bar strength in that case can be much less than in the case of a less elliptical bar in a bulge-less galaxy.

A quantitative observational measure of bar strength has recently been developed by Buta & Block (2001), based on an old of idea of Combes & Sanders (1981). Buta & Block calculate the maximum, Q_b, of the ratio of the tangential force to the mean axisymmetric radial force. Technically, this is done by a Fourier analysis of deprojected images, under the assumption of a constant mass-to-light ratio. This means that the observational input data must be NIR images with a high signal-to-noise ratio, which in turn implies a preference for bright, thus nearby, galaxies. This is where INGRID is ideal: the 4.2-m WHT mirror ensures a high S/N ratio, whereas the field of view of 4.2 arcmin facilitates the imaging of disks of nearby galaxies. We thus derived bar strengths, Q_b, for those galaxies in our sample of 57 galaxies where this could be determined (45 of them, the images of the others are not of high enough S/N ratio).

The galaxies in our sample were selected to have an angular diameter of more than 4.2 arcmin and an inclination of less than 50 degrees. Our sample covers the complete range in Hubble type for spiral galaxies, as well as in Elmegreen spiral arm class (Elmegreen & Elmegreen, 1987), from flocculent to grand-design. As an example, we show, in Figure 1, V and K_s-band images of the SA(rs)b galaxy Messier 88 (NGC 4501), where the V-band image was obtained with ING's 1-m JKT. This K_s-band image is one of our deepest, with a total on-source integration time of over one hour. The $V–K_s$ colour index image clearly shows the location of the star-forming spiral arms (as lighter shades) and the dust lanes which accompany them (darker).

4. Results

In Figure 2 we show nine of our sample galaxies, ranked in terms of increasing bar strength or torque. The locations where the ratio of the tangential force to the mean axisymmetric radial force reaches a maximum are indicated in each galaxy image by four filled black or yellow dots. Figure 3 shows a montage of K_s images of 9 two-armed spiral galaxies in our sample, ranked vertically in terms of bar torque, and horizontally in terms of pitch angle class, where class a contains the most tightly wound spirals.

Combining our results on the bar strength Q_b with those obtained by Buta & Block (2001) for 30 galaxies, we now have a sample of 75 galaxies with bar strengths determined from NIR imaging. In Figure 4, we plot the bar strength Q_b against the deprojected bar axis ratio, often used as a bar "strength" indicator, for those galaxies where the latter number has been published by Martin (1995). Whereas there is a general trend, as expected, where the most elongated bars (high

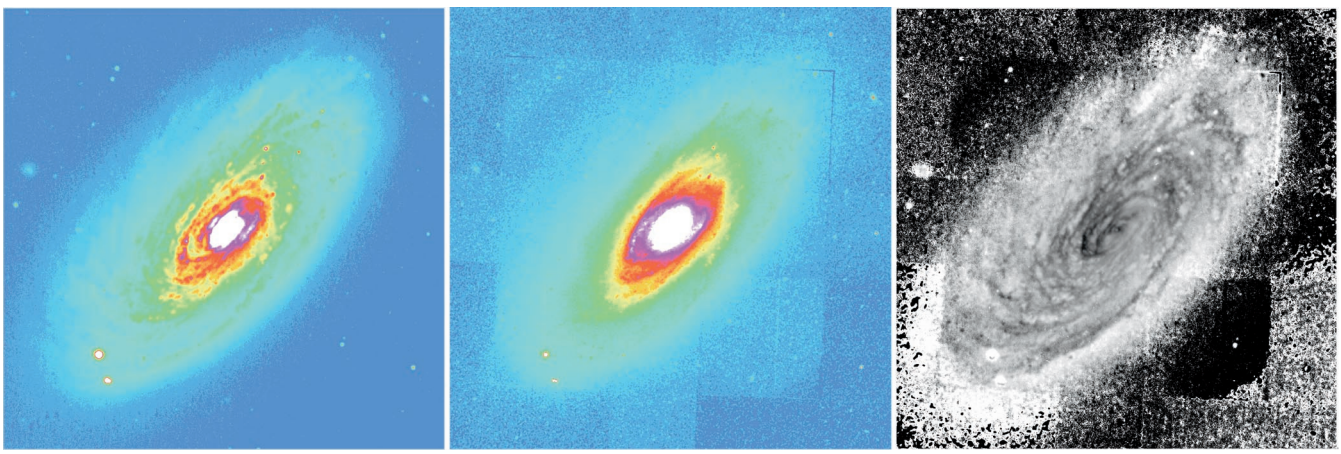

Figure 1. V, K_s, and $V–K_s$ colour index images of the SA(rs)b galaxy Messier 88 (NGC 4501), as obtained with INGRID on the WHT and with the JKT. The field of view of the images is ~7 arcmin, but only the central 4 arcmin is shown here.

ellipticity or axis ratio) also have the highest bar torques or strengths, the spread in Q_b for each axis ratio is very large, and in fact large enough as to invalidate any claims that bar ellipticity is a reliable bar strength estimator. For example, bars with moderate ellipticity (axis ratios of 0.4–0.5) span the entire range of bar strengths Q_b and their ellipticities are thus completely useless to discriminate strong from weak bars. It is only at the very extreme ends of the bar axis ratio range that such a discrimination might have a chance of success. Laurikainen, Salo & Rautiainen (2002) derive Q_b using a slightly different method, and compare their values with bar ellipticities. They find a better correlation between Q_b and bar axis ratio than we do, possibly due to the fact that the latter were derived from NIR images, whereas Martin (1995) used blue light photographs.

In Figure 5, we plot Q_b for each galaxy against its classification from de Vaucouleurs (1963), who classified galaxies as un-barred (SA), barred (SB) or intermediate (SAB, often referred to as weakly barred though this may not be correct in all cases). A clear trend is seen where the SB galaxies have higher bar strengths Q_b than SA or SAB galaxies, but more interesting is the considerable overlap in Q_b values between the SA, SAB and SB classes. This implies that many of the galaxies classed as SAB in fact have stronger bars than many classed SB, and even that a considerable number of SAB galaxies have weaker bars than others classed as un-barred! In addition, Figure 5 shows clearly that the effect of overlapping bar strength is not due to either early- or late-type galaxies, but is present equally for all sub-types. Massive bulges, which will dilute bar strength, are thus not the cause of the observed effect. Apparently, the relative bar strength comes from a complex mixture of bar amplitude, radial profile and relative length, combined with the bulge strength. The resulting spread of Q_b for each Hubble subtype is due to the different ways in which these quantities vary along the Hubble sequence. How exactly this affects

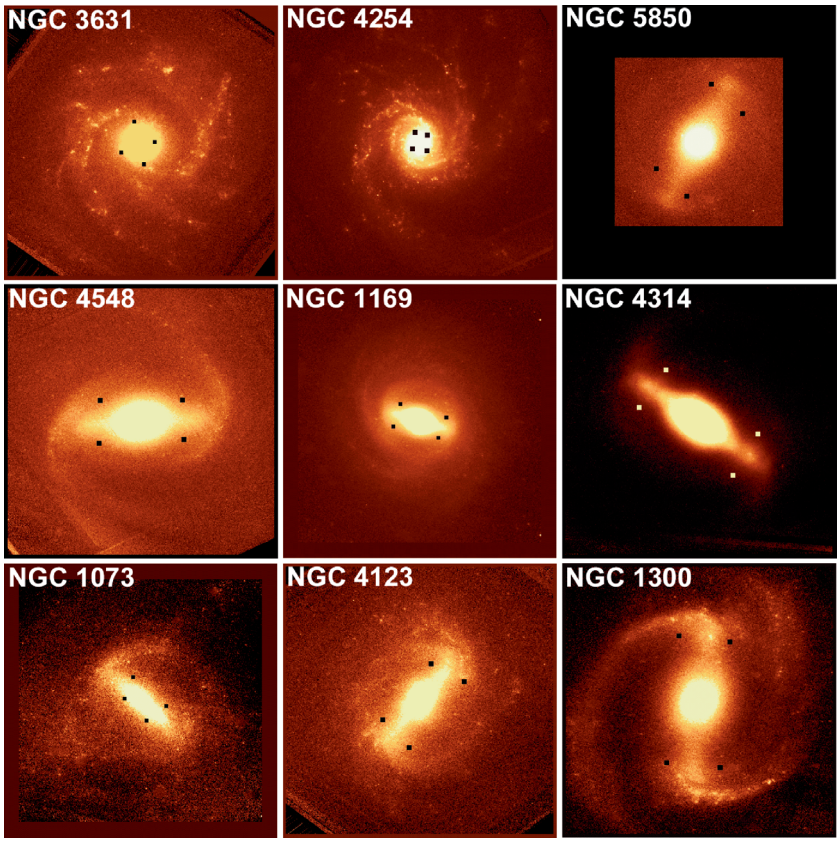

Figure 2. Deprojected K_s images of nine galaxies observed with the 4.2-m WHT, ranked in terms of increasing bar strength, or torque. The four filled black or yellow dots indicate the locations where the ratio of the tangential force to the mean axisymmetric radial force reaches a maximum. From Block et al. (2001).

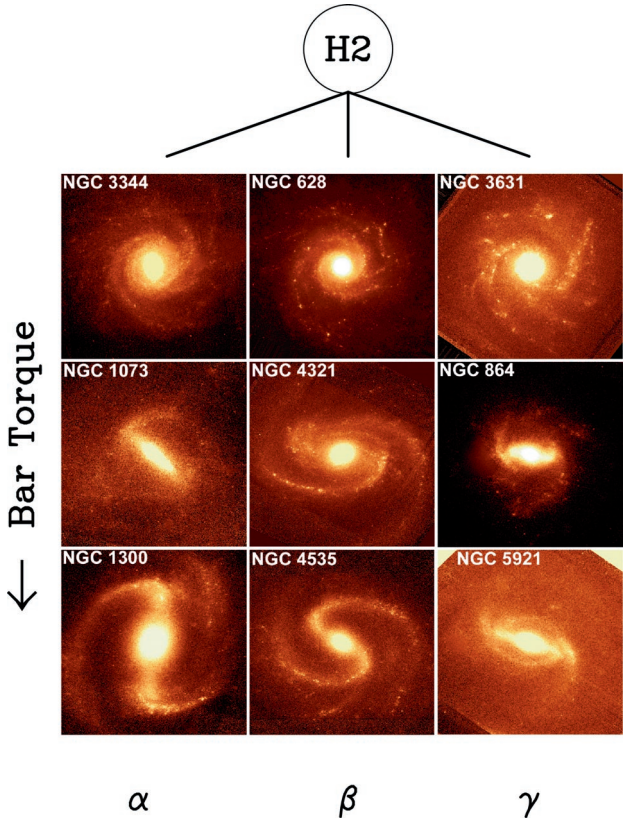

Figure 3. Montage of 9 K_s images of two-armed spirals, which have been ranked vertically in terms of bar torque, where the strongest bars are seen in the lower panels, and horizontally in terms of pitch angle class, where class α contains the most tightly wound spirals. From Block et al. (2001).

the bar parameters, and the influence the bar has on its surroundings, is not clear, and is the subject of our further exploration, partly aided by INGRID imaging.

5. Summary

In this short paper, we illustrate the power of the INGRID NIR camera on the WHT in obtaining deep, wide-field, imaging of nearby spiral galaxies. We describe results from our study of bar torques, or bar strengths, in a large sample of galaxies which we imaged with INGRID, and show that this bar strengths only very weakly correlates with de Vaucouleurs bar type, or with bar axis ratio.

References:

Block, D. L. & Wainscoat, R. J., 1991, *Nature*, **353**, 48.

Block, D. L., Bertin, G., Stockton, A., Grosbol, P., Moorwood, A. F. M., Peletier, R. F., 1994, *A&A*, **288**, 365.

Block, D. L., Puerari, I., Knapen, J. H., Elmegreen, D. M., Buta, R., Stedman, S., Elmegreen, D. M., 2001, *A&A*, **375**, 361.

Buta, R. & Block, D. L., 2001, *ApJ*, **550**, 243.

Combes, F. & Sanders, R. H., 1981, *A&A*, **96**, 164.

de Vaucouleurs, G., 1963, *ApJS*, **8**, 31.

Elmegreen, D. M. & Elmegreen, B. G., 1987, *ApJ*, **314**, 3.

Eskridge, P. B. et al., 2000, *AJ*, **119**, 536.

Knapen, J. H., 1999, in The Evolution of Galaxies on Cosmological Timescales, J. E. Beckman & T. J. Mahoney, Eds., *ASP Conf. Ser.*, **187**, 72.

Knapen, J. H., Shlosman, I. & Peletier, R. F., 2000, *ApJ*, **529**, 93.

Laurikainen, E., Salo, H. & Rautiainen, P., 2002, *MNRAS*, in press (astro-ph/0111376).

Martin, P., 1995, *AJ*, **109**, 2428.

Mulchaey, J. S., & Regan, M. W., 1997, *ApJ*, **482**, L135.

Sellwood, J. A. & Wilkinson, A., 1993, *Rep. Prog. Phys.*, **56**, 173. ¤

Johan Knapen (knapen@star.herts.ac.uk)

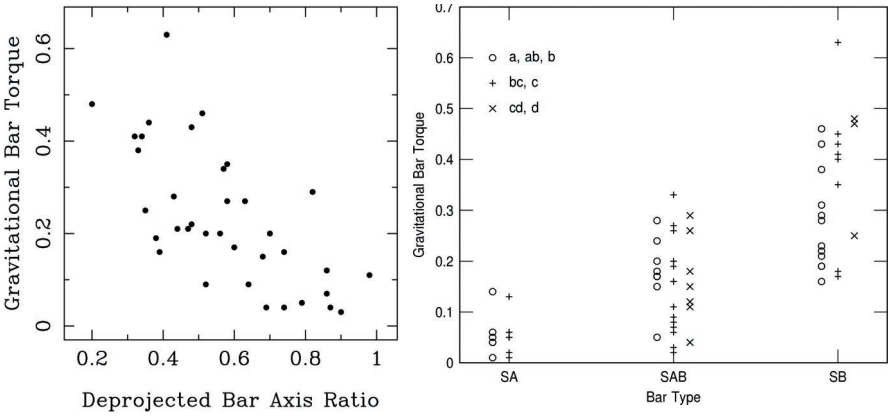

Figure 4 (left). Bar strength plotted as a function of deprojected bar ellipticity, or bar axis ratio. From Block et al. (2001). Figure 5 (right). Bar strength plotted as a function of Hubble type for our sample galaxies. From Block et al. (2001).

Searching for Obscured Supernovae in Nearby Starburst Galaxies

Seppo Mattila (Imperial College), Robert Greimel (ING), Peter Meikle (Imperial College), Nicholas A. Walton (IoA), Stuart Ryder (AAO), Robert D. Joseph (IfA)

We are currently carrying out a K_s band survey for core-collapse supernovae (CCSNe) in the nuclear (central kpc) regions of nearby starburst galaxies with the INGRID near-IR camera at the WHT. In this article we concentrate on describing mainly the observations and the real time processing of the SN search data, which makes use of the ING's integrated data flow system.

Very little is currently known about the behaviour of SNe in a starburst environment. The enhanced metallicity in starburst regions is expected to result in large mass-loss rates (Vink et al., 2001) for the SN progenitor stars. In addition, many of these events are expected to occur within molecular clouds (Chevalier & Fransson, 2001), adding further to the density of material surrounding the SN. Therefore, nuclear SNe can be expected to explode within a dense circumstellar medium. In general, a dense (but non-nuclear) circumstellar environment has been observed to produce bright CCSNe with slow near-IR light decline rates (e.g. SN 1998S, Fassia et al., 2000). However, the behaviour of SNe in nuclear starburst regions may be much more extreme (Terlevich et al., 1992). The high-z CCSN surveys with the VLT, HST and NGST (e.g., Dahlen & Fransson, 1999; Sullivan et al., 2000) will use SNe to probe the cosmic star formation rate. For this, it is important to determine (i) a better estimate of the *complete* local CCSN rate (cf. Sullivan et al., 2000), (ii) a proper understanding of the behaviour of SNe within the dusty, high-density starburst environment and (iii) the extinction towards these events.

Most of the CCSNe in young starbursts like M 82 (Figure 1; Mattila & Meikle, 2001, 2002) are expected to be heavily obscured by dust, and therefore remain undiscovered by current SN search programmes working at optical wavelengths. However, in the near-IR K_s-band the extinction is greatly reduced and the sensitivity of ground-based observations is still good. That is why we are using INGRID to carry out an imaging survey of the